Stability of Shock Waves Attached to Wedges and Cones

M. D. Salas*
NASA Langley Research Center, Hampton, Virginia
and
B. D. Morgan†
Iowa State University, Ames, Iowa

A numerical study of a reduced set of the Euler equations shows that both weak and strong attached shock waves are stable configurations depending on the boundary conditions imposed. The results obtained are in good agreement with experimental observations and with the minimum entropy principle. A heuristic explanation of the behavior observed is given in terms of quasistatic considerations.

Introduction

FOR flow over a wedge or cone, whose deflection angle is less than the angle associated with shock detachment for the incoming supersonic flow, it is a well-known fact that the steady-state Euler equations admit two different solutions. Each solution is distinguished by the strength of the attached oblique shock. Thus a solution is labeled *strong* or *weak* if the shock-wave inclination is, respectively, greater than or less than the shock-wave inclination at detachment. For the strong shock solution, the flow is always subsonic downstream of the shock; for the weak shock solution, the flow is supersonic downstream of the shock, except for a small range of deflection angles in the neighborhood of the detachment angle where the weak shock is followed by subsonic flow. This small region will be ignored in the present work. The existence of multiple solutions has attracted considerable theoretical scrutiny, which has mainly succeeded in obscuring the problem. Indeed, our understanding of this problem has changed little since 1948, when Courant and Friedrichs[1] wrote

> ...The question arises which of the two actually occurs. It has frequently been stated that the strong one is unstable and that, therefore, only the weak one could occur. A convincing proof of this instability has apparently never been given. Quite aside from the question of stability, the problem of determining which of the possible shocks occurs cannot be formulated and answered without taking the boundary conditions at infinity into account.

The confusion has come about because the question posed by Courant and Friedrichs and every succeeding investigator has not been the proper question to ask. The question should not be which solution actually occurs, since we have experimental evidence[2] that both the weak and the strong solutions do occur, but under what conditions do one or the other solutions occur. The answer to this latter question obviously depends on the boundary conditions, as already indicated by Courant and Friedrichs. Moreover, since the nature of steady-state solution is elliptic for the strong shock and hyperbolic for the weak shock, we should suspect that each problem is governed by a different set of boundary conditions.

The purpose of this paper is, therefore, to study the stability of the weak and strong solutions with boundary conditions which are appropriate to each case under investigation.

Historical Background

In 1931, Epstein[3] considered the problem with a variational formulation. Epstein argued, on the basis of Hamilton's principle and without taking the boundary conditions into account, that the strong-shock solution was unstable. This line of attack was, however, fundamentally wrong, because the variational formulation is valid only for reversible processes with no entropy creation,[4] which is not the case here.

A more rigorous investigation was presented by Carrier,[5] who studied the solutions admissible by the linearized time-dependent Euler equations subject to linearized Rankine-Hugoniot jumps at the shock and vanishing of the normal velocity component at the wall. These boundary conditions are consistent with the hyperbolic nature of the steady-state weak solution, since no downstream boundary condition is imposed. Although Carrier's work did not show how an arbitrary initial disturbance grows with time, he concluded, partially based on his knowledge that the strong shock has been observed experimentally, that both the weak and strong shock solutions are stable. As will be shown later, for the boundary conditions that Carrier imposed, only the weak solution is stable.

Recently, Henderson and Atkinson,[6] apparently unaware of the theoretical work of Carrier and of the experimental findings, presented a linear analysis of the problem where, again, they considered only boundary conditions similar to those applied by Carrier. Their analysis, however, correctly showed that under this set of boundary conditions only the weak solution is stable. From this, they concluded that the strong shock solution is unstable, failing to realize that this

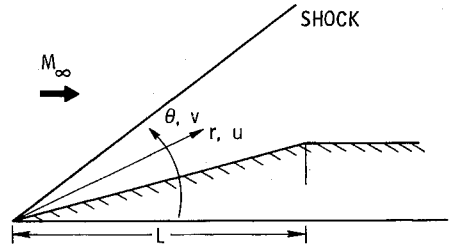

Fig. 1 Spherical coordinates system used for wedge and cone calculations.

Presented as Paper 82-0288 at the AIAA 20th Aerospace Sciences Meeting, Orlando, Fla., Jan. 11-14, 1982; submitted Jan. 22, 1982; revision received March 22, 1983. This paper is declared a work of the U.S. Government and therefore is in the public domain.

*Research Scientist, TAB, TAD. Associate Fellow AIAA.
†Research Assistant. Student Member AIAA.

other solution could be stable under a different set of boundary conditions.

The latest work on this problem has been conducted by Rusanov and Sharakshanae,[7] who again considered only the boundary conditions imposed by the previous workers and arrived at the same conclusion as Henderson and Atkinson. This latest investigation did not linearize the governing equations, instead it studied numerically the exact time-dependent equations under the assumption of conicity. This will be the approach we will follow in our investigation.

Principle of Minimum Entropy

Before embarking on our study of this problem, it will be elucidating to introduce at this stage the a posteriori axiom known as the principle of minimum entropy production.[8] This principle, which cannot be proven for the nonlinear equations under investigation, has been found to accurately predict the stability of a wide range of phenomena. It states that, if more than one steady state is compatible with the prescribed boundary conditions, the state that will be observed is that with the minimum value of entropy. The principle is helpful to the theoretician in discriminating spurious solutions when more than one mathematically admissible solution exists; nature, on the other hand, need no help. A cursory application of this principle would seem to indicate that the strong shock solution would be discarded, since it has a higher value of entropy associated with it than the weak solution. This appears to have been the line of thought of Henderson and Atkinson however, in what follows, it will be shown that the occurrence of the strong-shock solution is not inconsistent with the minimum entropy principle.

Formulation of the Problem

Consider a two-dimensional wedge or circular cone placed in a uniform supersonic flow with Mach number M_∞ and isentropic exponent γ and let the angle of the wedge or cone be less than the angle corresponding to shock detachment. Assuming an inviscid flow, the nondimensional equations governing the flow are

$$P_t+\frac{v}{r}P_\theta+uP_r+\gamma\left[\frac{v_\theta}{r}+u_r+\frac{u}{r}+\left(\frac{u}{r}+\frac{v}{r}\cot\theta\right)j\right]=0 \quad (1)$$

$$v_t+\frac{vv_\theta}{r}+uv_r+\frac{a^2}{\gamma r}P_\theta+\frac{uv}{r}=0 \quad (2)$$

$$u_t+\frac{vu_\theta}{r}+uu_r+\frac{a^2}{\gamma}P_r-\frac{v^2}{r}=0 \quad (3)$$

$$S_t+\frac{vS_\theta}{r}+uS_r=0 \quad (4)$$

where r and θ are spherical coordinates as indicated in Fig. 1; t is time; P stands for the natural logarithm of the pressure normalized by the freestream pressure; u and v are the radial and circumferential velocity components, respectively, normalized by the square root of the freestream pressure divided by the freestream density; S is the entropy normalized by the coefficient of specific heat at constant volume; and a is the speed of sound defined by

$$a^2=\gamma\exp\left(\frac{\gamma-1}{\gamma}P+\frac{S}{\gamma}\right) \quad (5)$$

In Eq. (1), the two-dimensional flow over a wedge is obtained by setting $j=0$, and the axisymmetric flow over a circular cone by setting $j=1$.

Sufficient boundary conditions for the hyperbolic (weak shock) problem are the Rankine-Hugoniot jumps at the shock and $v=0$ at the surface of the wedge or cone. For the elliptic (strong shock) problem, in addition to these boundary conditions, some condition far downstream must be imposed to properly close the problem. In the laboratory, in order to obtain the strong shock solution, the additional constraint imposed is the downstream pressure.[2] A simulation of this condition will be used to study the strong shock solution.

As the problem now stands, it is very difficult to attack numerically because of major difficulties arising in the numerical treatment of the apex. The problem, however, becomes tractable if the solution is assumed to be conically self-similar. For the time-dependent problem, this assumption is not valid globally. However, it is easy to prove that the assumption of conicity is valid in a small region near the apex of the wedge or cone. At a fixed radial location $r=r_0$, we rewrite Eqs. (1-4) after multiplying by r_0 and introducing the notation $t=\tau r_0$,

$$P_\tau+vP_\theta+r_0uP_r+\gamma[v_\theta+r_0u_r+u+(u+v\cot\theta)j]=0 \quad (6)$$

$$v_\tau+vv_\theta+r_0uv_r+(a^2/\gamma)P_\theta+uv=0 \quad (7)$$

$$u_\tau+vu_\theta+r_0uu_r+(a^2/\gamma)r_0P_r-v^2=0 \quad (8)$$

$$S_\tau+vS_\theta+r_0uS_r=0 \quad (9)$$

We now choose r_0 to be a sufficiently small radius near the apex such that the terms multiplied by r_0 in Eqs. (6-9) are small compared to the remaining terms. The resulting conical equations are

$$P_\tau+vP_\theta+\gamma[v_\theta+u+(u+v\cot\theta)j]=0 \quad (10)$$

$$v_\tau+vv_\theta+(a^2/\gamma)P_\theta+uv=0 \quad (11)$$

$$u_\tau+vu_\theta-v^2=0 \quad (12)$$

$$S_\tau+vS_\theta=0 \quad (13)$$

The conical assumption requires a re-examination of the boundary conditions. For the hyperbolic (weak shock) problem, it is still possible to impose the Rankine-Hugoniot jumps at the shock and $v=0$ at the wall. For the elliptic (strong shock) problem, it is possible to impose the Rankine-Hugoniot jumps at the shock and $v=0$ at the wall, but we can no longer impose the pressure level downstream, which is the critical boundary condition for the elliptic problem. It is, however, possible to require that a given pressure level be satisfied at the wall and to permit the wall to move in time. At each instant of time, it will, of course, be required that the normal velocity component relative to the wall be zero. Thus v will vanish at the wall as the steady state is reached asymptotically. To accomplish this, introduce computational coordinates ξ and η, defined by

$$\xi=\frac{\theta-\theta_w(\tau)}{\theta_s(\tau)-\theta_w(\tau)} \quad (14)$$

$$\eta=\tau \quad (15)$$

where $\theta_w(\tau)$ and $\theta_s(\tau)$ define the wall and shock locations in time. Recast Eqs. (10) and (11) in terms of computational coordinates and combine into the characteristic relation,

$$P_\eta+\lambda^\pm P_\xi\pm\frac{\gamma}{a}(v_\eta+\lambda^\pm v_\xi)=-\gamma\left[\frac{u}{a}(a\pm v)+(u+v\cot\theta)j\right] \quad (16)$$

which is valid along the characteristic directions

$$\lambda^\pm=\xi_\tau+\xi_\theta(v\pm a) \quad (17)$$

The characteristic reaching the wall has direction $\lambda^-=\xi_\tau+\xi_\theta(v-a)$. To satisfy the wall boundary condition for the hyperbolic problem, set v and v_η equal to zero (the wall location is fixed) in Eq. (16) and solve for the variation of pressure with time. For the elliptic problem, the pressure level

at the wall is fixed, which implies that P_η is zero in Eq. (16); it is then possible to solve for the wall acceleration v_η. These boundary conditions will be referred to as the fixed-wall and fixed-pressure boundary conditions, respectively. If a steady, stable solution exists, the equations of motion will reach this state asymptotically in time.

Numerical Integration of the Equations

The numerical integration of the equations follows standard procedures which have been discussed at length in the literature; see, for example, Ref. 9. Here it will be appropriate to give only a brief outline of the method.

The equations of motion (10-13) are written in terms of computational coordinates ξ and η. The recast counterparts of Eqs. (10) and (11) are then integrated using the MacCormack scheme, while the counterparts of Eqs. (12) and (13) are integrated uisng windward differences only. Note that both Eqs. (12) and (13) are singular at the wall, developing boundary-layer-like solutions if the wall is held fixed. This requires, in order to evaluate u and S at the wall, an extrapolation from inside the flowfield to the wall which models the collapse of the entropy and u layers after long times. In the numerical integration, the shock is allowed to move in time, satisfying at each time instant the Rankine-Hugoniot jumps and the compatibility relation [Eq. (16)] reaching the shock from the high-pressure side. The wall boundary condition requires that either the wall location be fixed or that the pressure level be fixed, and these boundary conditions are evaluated as previously discussed.

The flowfield is initialized with the exact solution corresponding to a wedge or cone with deflection angle a few degrees different from the case of interest. For the fixed-wall boundary condition, the wall is then slowly moved to the position of interest and the resulting transient is computed. For the fixed-pressure boundary condition, the pressure at the

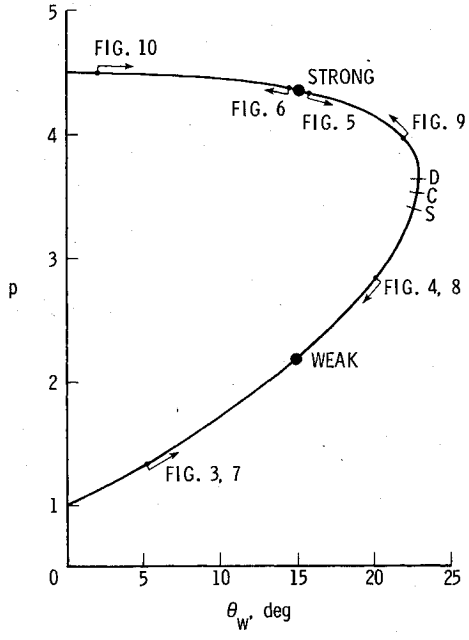

Fig. 2 Pressure shock polar for flow over a wedge at $M_\infty = 2$. Detachment, Crocco, and sonic points are marked on the polar. Cases described in the text are indicated on the polar by corresponding figure numbers. Arrows indicate convergence trend.

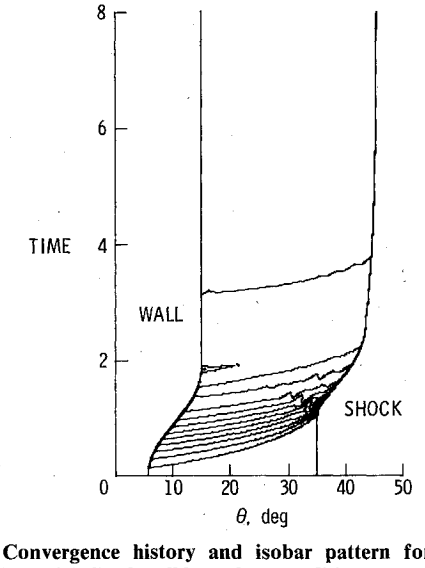

Fig. 3 Convergence history and isobar pattern for weak shock solution imposing fixed-wall boundary condition.

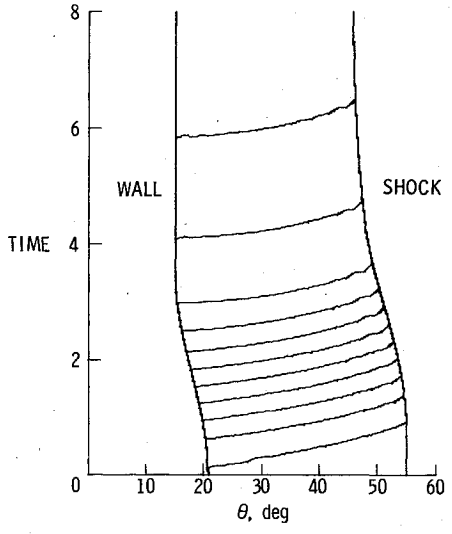

Fig. 4 Convergence history and isobar pattern for weak shock solution imposing fixed-wall boundary condition.

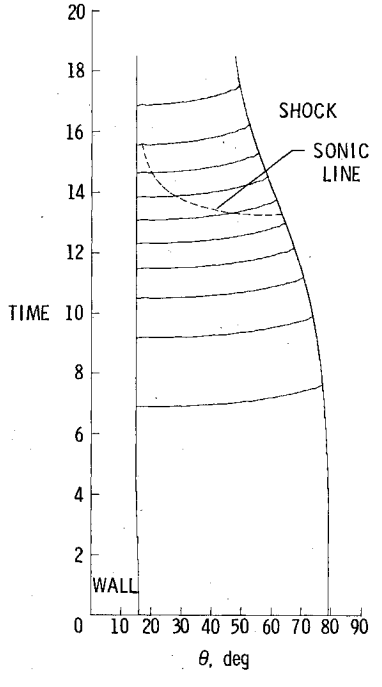

Fig. 5 Convergence history and isobar pattern for initially strong shock solution imposing fixed-wall boundary condition. Solution converges to weak shock solution.

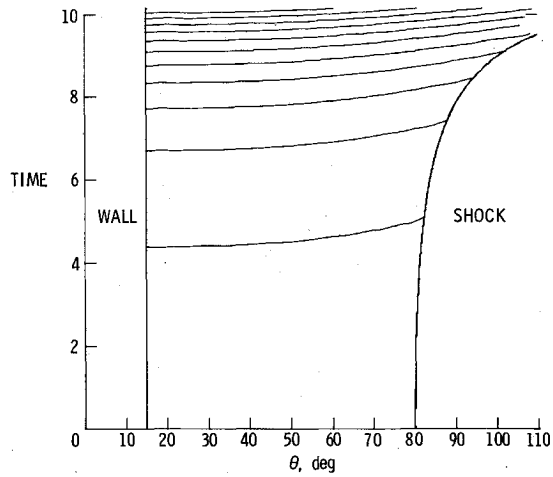

Fig. 6 Convergence history and isobar pattern for initially strong shock solution imposing fixed-wall boundary condition. Solution diverges as shock wave becomes increasingly stronger.

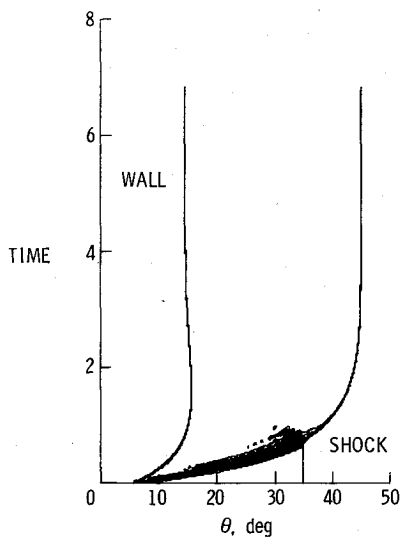

Fig. 7 Convergence history and isobar pattern for weak shock solution imposing fixed-pressure boundary condition.

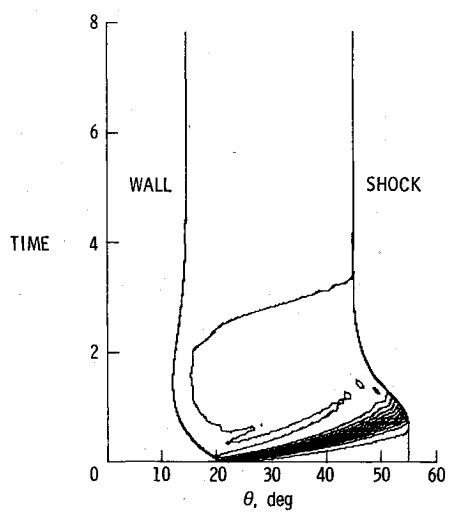

Fig. 8 Convergence history and isobar pattern for weak shock solution imposing fixed-pressure boundary condition.

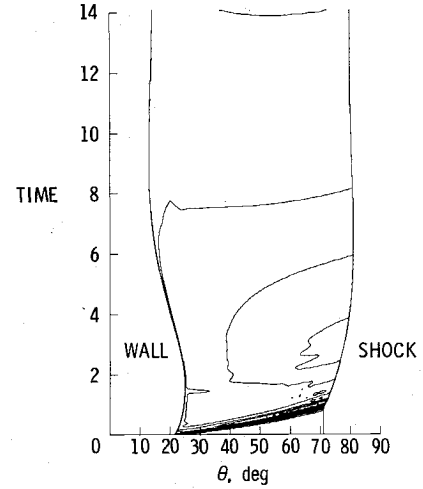

Fig. 9 Convergence history and isobar pattern for initially strong shock solution imposing fixed-pressure boundary condition. Solution converges to strong shock solution.

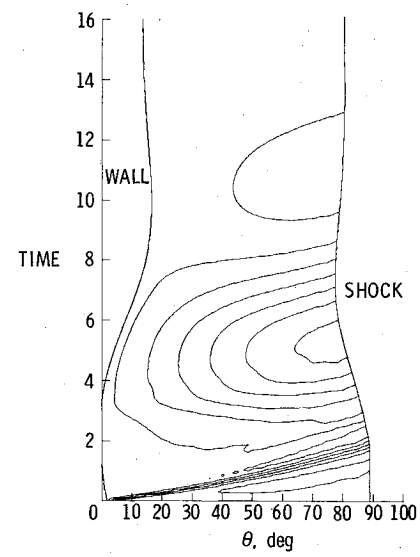

Fig. 10 Convergence history and isobar pattern for initially strong shock solution imposing pressure boundary conditions. Solution converges to strong shock solution.

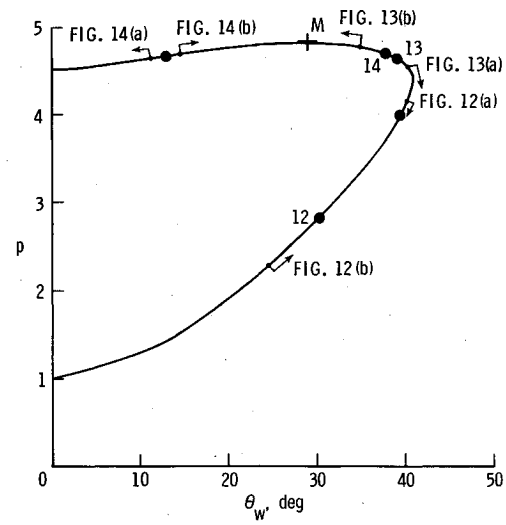

Fig. 11 Surface-pressure shock polar for flow over a cone at $M_\infty = 2$. Point M indicates maximum surface pressure. Cases described in the text are indicated on the polar by corresponding figure numbers. Arrows indicate convergence trend.

wall is discontinuously changed to the value of interest and the resulting transient is computed.

Numerical Results

Wedge

All cases investigated correspond to $M_\infty = 2$ and $\gamma = 1.4$. The pressure shock polar shown in Fig. 2 shows the two possible solutions at this Mach number for a 15-deg wedge; also shown in the figure are the sonic, Crocco, and detachment points, labeled S, C, and D, respectively. As can be seen from the figure, the surface pressure is a multivalued function of the wedge angle, but the wedge angle is a single-valued function of the pressure.

Figure 3 shows the time evolution of the flowfield resulting from initial conditions corresponding to a weak solution with wedge deflection angle slightly less than 15 deg. During a short transient ($t<2.0$), the wall is moved to a 15-deg inclination and is then held fixed; this sends a train of compression waves to the shock, which pushes it away from the wall and raises its pressure. As seen from the figure, the desired weak solution is obtained asymptotically. Figure 4 shows a similar time evolution resulting from initial conditions corresponding to slightly larger initial wedge deflection angle. Now a series of expansions are sent from the wall to the shock, lowering the shock pressure and pulling it closer to the wall. These results indicate that, for the wedge, the weak solution is stable for the fixed-wall boundary conditions.

Figure 5 shows the time evolution resulting from initial conditions corresponding to a strong-shock solution with a wedge inclination initially a little larger than 15 deg. As is evident from the figure, as the body inclination decreases, expansion waves are sent from the body to the shock, pulling the shock closer to the body and lowering its pressure. The solution then converges asymptotically to the previous weak shock solution. Figure 6 shows the time evolution resulting from initial conditions corresponding to a strong-shock solution with a wedge inclination initially slightly less than 15 deg. As the figure shows, compression waves are sent from the wall to the shock, pushing it away from the wall and raising its pressure. A reinforcing mechanism is set up, and the solution does not converge to a steady state. These examples show that for a wedge the strong solution is unstable for the fixed-wall boundary conditions; this was basically the extent of the work of Rusanov and Sharakshanae.[7]

Consider now what happens if the fixed-pressure boundary condition is used. The results are shown in Figs. 7-10, which are the equivalent of the previous four figures. As is evident from these figures, both the weak and strong-shock solutions for a wedge are stable for this boundary condition.

Cone

The shock polar for a cone is shown in Fig. 11. Figure 12 depicts the time evolution resulting from initial conditions in the neighborhood of the weak solution of interest (30-deg cone) and using the fixed-wall boundary condition. As is evident from the figure, the solutions asymptotically reach a stable, steady state.

As in the case of the wedge, the strong solution is unstable for this boundary condition, as shown in Fig. 13. Here again, if the initial conditions correspond to a slightly greater cone inclination than that of the case of interest (39 deg for this case), the solution converges to the weak solution. If the initial cone inclination is less than that of the case of interest, then the solution diverges.

The weak solution for a cone, again, is stable with the fixed-pressure boundary condition. The strong solution, however, needs closer investigation. As shown in Fig. 11, the

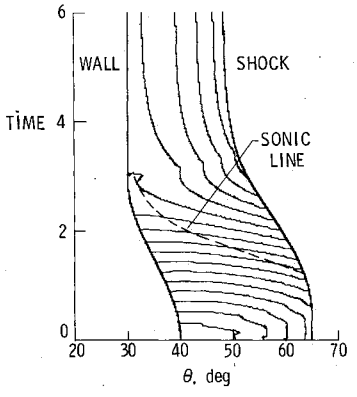

Fig. 12a Convergence history and isobar pattern for weak shock solution imposing fixed-wall boundary conditions. Although initial conditions correspond to subsonic flow, they still lie within weak shock branch.

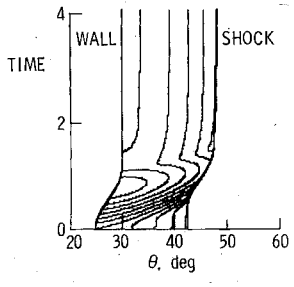

Fig. 12b Convergence history and isobar pattern for weak shock solution imposing fixed-wall boundary condition.

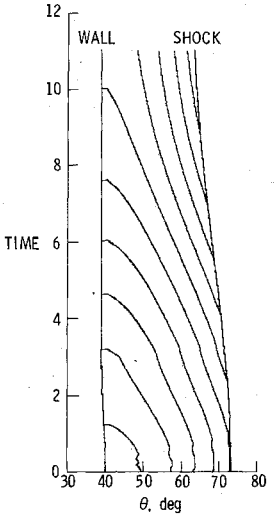

Fig. 13a Convergence history and isobar pattern for initially strong shock solution imposing fixed-wall boundary condition. Solution converges to weak shock solution.

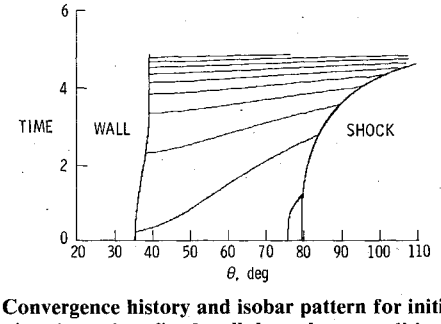

Fig. 13b Convergence history and isobar pattern for initially strong shock solution imposing fixed-wall boundary condition. Solution diverges as shock wave becomes increasingly stronger.

strong-shock branch of the shock polar for a cone has a different behavior than the strong-shock branch for a wedge (Fig. 2). This behavior occurs because the value of the pressure behind a normal shock (resulting in no flow deflection) is the same at the shock and at the surface of the zero deflection cone; but, for any other cone deflection, the surface pressure is higher than the pressure at the shock. A consequence of this is that, for a given surface pressure, there exist multiple values of the cone deflection angle. The numerical results showed that, when a value of surface pressure was specified between its maximum value (point M in Fig. 11) and its value for a normal shock, the stable solution was that corresponding to cone deflections greater than the cone deflection corresponding to maximum surface pressure. An example is shown in Fig. 14. This figure shows the time evolution corresponding to a fixed surface pressure of 4.675, which can be satisfied by a 12 deg or a 38.35-deg cone. Figure 14a corresponds to initial conditions for a cone inclination slightly less than 12 deg, and Fig. 14b corresponds to initial conditions for a cone inclination slightly greater than 12 deg. The first case diverges, while the latter converges to the 38.35-deg cone inclination solution.

Principle of Minimum Entropy—Revisited

To understand why a stable strong shock solution does not necessarily contradict the minimum entropy principle, it must be remembered that the principle applies when multiple steady states occur that satisfy the same boundary conditions. Thus, for a wedge and the fixed wall boundary condition (θ_w given), there are two possible solutions, one with a value of pressure lower than the other, as is evident from Fig. 2. The principle correctly predicts that, for this case (this set of boundary conditions), only the weak solution is stable. However, if the pressure is given as a boundary condition, then there is only one solution admissible (a unique wedge angle that satisfies that pressure), thus the minimum entropy principle is not required.

For the circular cone, again, the minimum entropy principle prediction agrees with the numerical results. Here, for the strong shock solution, a given surface pressure level could result in multiple values of cone angles (see Fig. 11). The stable solution predicted by the principle is the one with minimum entropy (larger cone deflection), in agreement with the numerical results.

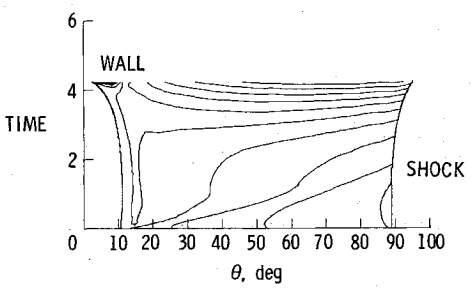

Fig. 14a Convergence history and isobar pattern for strong-shock solution imposing fixed-pressure boundary condition. Solution diverges as shock wave becomes increasingly stronger.

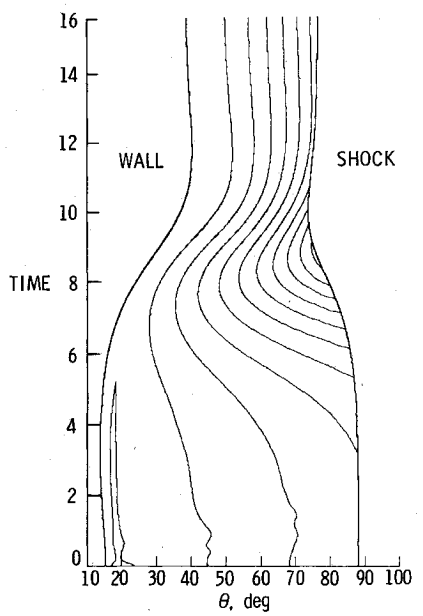

Fig. 14b Convergence history and isobar pattern for strong shock solution imposing fixed-pressure boundary condition. Solution converges to strong shock solution with minimum entropy.

Quasistatic Analysis

In this section, we will complete an analysis initiated but not quite completed by Henderson and Atkinson.[6] The analysis is heuristic and is presented for the two-dimensional wedge only. The stability of the weak shock solution is explained by coupling the behavior of the pressure and streamline inclination at the shock to the boundary condition at the surface. For the strong shock solution, because of the subsonic nature of the flow, we must resort to a consideration of the behavior of the streamline curvature between the shock and the surface. Although the latter considerations could also be used to explain the weak shock behavior, they do not seem quite as convincing as the argument presented here.

With reference to Fig. 15, the pressure and flow inclination at the shock are given by the Rankine-Hugoniot relations

$$\frac{p_s}{p_\infty} = \frac{2\gamma M_\infty^2 \sin^2\omega}{\gamma+1} - \frac{\gamma-1}{\gamma+1} \tag{18}$$

$$\cot\delta_s = \left[\frac{\frac{1}{2}(\gamma+1)M_\infty^2}{M_\infty^2\sin^2\omega - 1}\right]\tan\omega \tag{19}$$

If we consider a small, quasistatic change in the shock inclination, $\Delta\omega$, the corresponding changes in the pressure and streamline inclination at the shock are

$$\frac{\Delta p_s}{p_\infty} = \frac{4\gamma}{\gamma+1} M_\infty^2 (\sin\omega\cos\omega)\Delta\omega \tag{20}$$

$$\Delta\delta_s = -\frac{\sin\delta_s\cos\delta_s}{\sin\omega\cos\omega} \times \left[1 - \frac{(\gamma+1)M_\infty^4\sin^2\omega\cos^2\omega}{(M_\infty^2\sin^2\omega - 1)\{1+[(\gamma+1)/2]M_\infty^2 - M_\infty^2\sin^2\omega\}}\right]\Delta\omega \tag{21}$$

Equation (20) shows that, for both the weak and strong shocks, a small increase in the shock inclination produces an increase in the pressure behind the shock. The quantity in the large brackets in Eq. (21) says that, for the weak shock, a small increase in the shock inclination results in an increase in the flow deflection; but, for the strong shock, a small increase

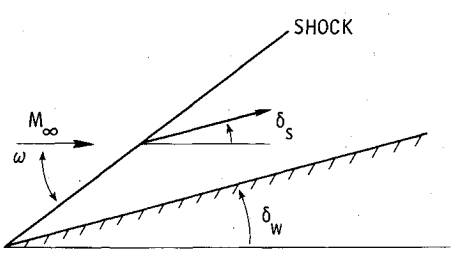

Fig. 15 Parameters used in quasistatic analysis of Rankine-Hugoniot equations.

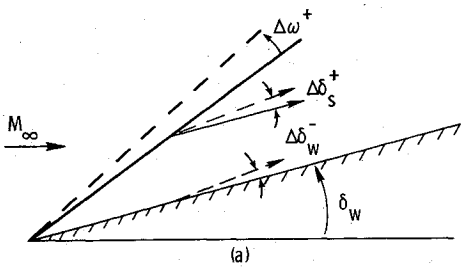

Fig. 16a Change in streamline inclination, δ_s, at a weak-shock wave due to a $\Delta\omega^+$ change in shock inclination, and corresponding turn $\Delta\delta_w^-$ needed to satisfy tangency condition.

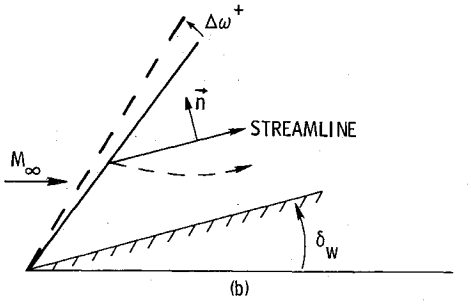

Fig. 16b Change in shape of streamline due to a $\Delta\omega^+$ change in the inclination of a strong-shock wave.

in the shock inclination results in a decrease in the flow deflection. In summary,

$\Delta\omega > 0 \rightarrow \Delta p_s > 0$ for weak and strong shocks

$\Delta\omega > 0 \rightarrow \begin{cases} \Delta\delta > 0 & \text{for weak shocks} \\ \Delta\delta < 0 & \text{for strong shocks} \end{cases}$

For the weak shock, the flow is supersonic downstream of the shock and the pressure at the wall is given by[10]

$$\Delta p_w \cong \Delta\delta_w / \sqrt{M_0^2 - 1} \tag{22}$$

where M_0 is the Mach number behind the shock. For the fixed-wall boundary condition, a small increase in the shock inclination, $\Delta\omega^+$, produces an increase in flow deflection at the shock, $\Delta\delta_s^+$, as indicated in Fig. 16a. This deflection must be brought back parallel to the wall, producing [according to Eq. (22)] a negative pressure increment at the wall which tends to balance the pressure increase at the shock and makes the weak shock stable.

For the strong shock, we can relate the pressure gradient normal to the streamlines to the streamline curvature, $\partial\delta/\partial s$, by[10]

$$\frac{\partial p}{\partial n} = -\gamma p M_0^2 \frac{\partial \delta}{\partial s} \tag{23}$$

An increase in the shock inclination, $\Delta\omega^+$, produces a decrease in the streamline inclination, $\Delta\delta_s^-$, at the shock. The streamline must then turn as indicated in Fig. 16b in order to satisfy the surface tangency condition. This requires that $\partial\delta/\partial s$ be greater than zero; and therefore, from Eq. (23), the pressure increases toward the wall. The increase in pressure at the wall reinforces the pressure increase at the shock and makes the strong shock unstable.

Since a constant pressure boundary reflects waves with the opposite sign, it follows that, for the fixed pressure boundary condition, a restoring force is produced at the wall for both the weak- and strong-shock solutions that renders both solutions stable.

Conclusions

The numerical results and the quasistatic analysis showed that the weak-shock solution is the only stable solution for the fixed-wall boundary condition. This agrees with the many experimental observations made for wedges and cones in free air and with prior theoretical work. For a wedge, the numerical results and the quasistatic analysis showed that both the weak- and strong-shock solutions are stable if the pressure is imposed as a boundary condition, in agreement with experimental observations made on inlets. For cones, the numerical results revealed an unstable region for the strong-shock branch and the fixed-pressure boundary condition. All the results were shown to be consistent with the predictions of the minimum entropy principle.

Acknowledgments

The authors are indebted to J. C. South Jr., of Langley Research Center and D. A. Anderson of Iowa State University for many fruitful discussions during the course of this study.

References

[1] Courant, R. and Friedrichs, K. D, *Supersonic Flow and Shock Waves*, Interscience Publishers, Inc., New York, 1948, p. 317.

[2] Shapiro, A. H., *The Dynamics and Thermodynamics of Compressible Fluid Flow*, The Ronald Press Co., New York, 1953, p. 547.

[3] Epstein, P. S., "On the Air Resistance of Projectiles," *Proceedings of the National Academy of Science*, Vol. 17, 1931, pp. 532-547.

[4] Herivel, J. W., "The Derivation of the Equations of Motion of an Ideal Fluid by Hamilton's Principle," *Proceedings of the Cambridge Philosophical Society*, Vol. 51, Pt. 2, 1955, pp. 344-349.

[5] Carrier, G. F., "On the Stability of the Supersonic Flows Past a Wedge," *Quarterly of Applied Mathematics*, Vol. 6, 1949, pp. 367-378.

[6] Henderson, L. F. and Atkinson, J. D., "Multi-Valued Solutions of Steady-State Supersonic Flow. Part 1. Linear Analysis," *Journal of Fluid Mechanics*, Vol. 75, Part 4, 1976, pp. 751-764.

[7] Rusanov, V. V. and Sharakshanae, A. A., "On the Non-Uniqueness of the Solution of the Problem on Steady Flow About the Plane Wedge and Circular Cone," *Computers and Fluids*, Vol. 8, 1979, pp. 243-250.

[8] Glansdorff, P. and Prigogine, I., *Thermodynamic Theory of Structure, Stability and Fluctuations*, John Wiley and Sons, Ltd., London, 1971, pp. 34-38.

[9] Salas, M. D., "Careful Numerical Study of Flowfields About Symmetric External Corners," *AIAA Journal*, Vol. 18, June 1980, pp. 646-651.

[10] Liepmann, H. W. and Roshko, A., *Elements of Gasdynamics*, John Wiley and Sons, Inc., New York, 1957, pp. 208-216.